
Causal Policy Gradients: Leveraging Structure for Efficient Learning in (Factored) MOMDPs

Thomas Spooner
J. P. Morgan AI Research
thomas.spooner@jpmorgan.com

Nelson Vadori
J. P. Morgan AI Research
nelson.vadori@jpmorgan.com

Sumitra Ganesh
J. P. Morgan AI Research
sumitra.ganesh@jpmorgan.com

Abstract

Policy gradient methods can solve complex tasks but often fail when the dimensionality of the action-space or objective multiplicity grow very large. This occurs, in part, because the variance on score-based gradient estimators scales quadratically. In this paper, we address this problem through a causal baseline which exploits independence structure encoded in a novel action-target influence network. Causal policy gradients (CPGs), which follow, provide a common framework for analysing key state-of-the-art algorithms, are shown to generalise traditional policy gradients, and yield a principled way of incorporating prior knowledge of a problem domain’s generative processes. We provide an analysis of the proposed estimator and identify the conditions under which variance is reduced. The algorithmic aspects of CPGs are discussed, including optimal policy factorisation, as characterised by minimum biclique coverings, and the implications for the bias-variance trade-off of incorrectly specifying the network. Finally, we demonstrate the performance advantages of our algorithm on large-scale bandit and traffic intersection problems, providing a novel contribution to the latter in the form of a spatio-causal approximation.

1 Introduction

Many sequential decision-making problems in the real-world have objectives that can be naturally decomposed into a set of conditionally independent targets. Control of water reservoirs, energy consumption optimisation, market making, cloud computing allocation, sewage flow systems, and robotics are but a few examples [36]. While many optimisation methods have been proposed [25, 34] — perhaps most prominently using Lagrangian scalarisation [45] — multi-agent learning has emerged as a promising new paradigm for effective learning [6]. In this class of algorithms, the multi-objective learning problem is cast into a centralised, co-operative stochastic game in which co-ordination is achieved through global coupling terms in each agent’s objective/reward functions. For example, a grocer who must manage their stock could be decomposed into a collection of daemon agents that each manage a single type of produce, but are subject to a global constraint on inventory. This approach has been shown to be very effective in a number of domains [20, 49, 30, 24, 51], but presents both conceptual and technical issues.

The transformation of a multi-objective Markov decision process (MOMDP) [36] into a stochastic game is a non-trivial design challenge. In many cases there is no clear delineation between agents in the new system, nor an established way of performing the decomposition. What’s more, it’s unclear in many domains that a multi-agent perspective is appropriate, even as a technical trick. For example, the concurrent problems studied by Silver et al. [39] exhibit great levels of homogeneity,

lending themselves to the use of a shared policy which conditions on contextual information. The key challenge that we address in this paper is precisely how to scale these single-agent methods — specifically, policy gradients — in a *principled* way. As we shall see, this study reveals that existing methods in both single- and multi-agent multi-objective optimisation can be formulated as special cases of a wider family of algorithms we entitle *causal policy gradients*. The contributions of this paper are summarised below:

1. We introduce *influence networks* as a framework for modelling causal relationships between actions and objectives in an MOMDP, and show how they can be combined with *policy factorisation* via graph partitioning.
2. We propose a *causal baseline* that exploits independence structures within a (factored) influence network, and show how this gives rise to a novel class of algorithms to which we ascribe the name *causal policy gradients*.
3. We show that CPGs *generalise traditional policy gradient estimators* and provide a common framework for analysing state-of-the-art algorithms in the literature including action-dependent baselines and counterfactual policy gradients.
4. The *variance properties* of our family of algorithms are studied, and *minimum factorisation* is put forward as a principled way of applying CPGs, with theoretical results around the existence and uniqueness of the characterisation.
5. The final contribution is to illustrate the effectiveness of our approach over traditional estimators on two *high-dimensional benchmark domains*.

1.1 Related Work

Policy gradients. Variance reduction techniques in the context of policy gradient methods have been studied for some time. The seminal work of Konda and Tsitsiklis [19] was one of the earliest works that identified the use of a critic as beneficial for learning. Since then, baselines (or, control variates) have received much attention. In 2001, Weaver and Tao [52] presented the first formal analysis of their properties, and later Greensmith et al. [13] proved several key results around optimality. More recently, these techniques have been extended to include action-dependent baselines [46, 22, 12, 56, 9], though the source of their apparent success has been questioned by some [48] who suggest that subtle implementation details were the true driver. It has also been shown that one can reduce variance by better accounting for the structure of the action-space, such as bounds [4, 10] or more general topological properties [7]. The SVRPG approach of Papini et al. [29] also addresses variance concerns in policy gradients by leveraging advances in supervised learning, and the generalised advantage estimator of Schulman et al. [37] has been proposed as a method for reducing variance in actor-critic methods with fantastic empirical results; both of these can be combined with baselines and the techniques we present in this work. **Factorisation.** In a related, but distinct line of work, factorisation has been proposed to better leverage the structure of MDPs; see e.g. [2, 15, 44]. Indeed, the notion of causality has been utilised similarly in work by Jonsson and Barto [16]. Most recently, Oliehoek et al. [27] presented an elegant framework for harnessing the *influence* of other agents (from the perspective of self) in multi-agent systems. This approach is complementary to the work presented in this paper, and more recent extensions have significantly advanced the state-of-the-art [41, 5, 28]; we build upon these principles. **Miscellaneous.** Causal/graphical modelling has seen past applications in RL [11]. Indeed, our proposed influence network is related to, but distinct from, the action influence models introduced by Madumal et al. [23] for explainability. There, the intention was to construct policies that can justify actions with respect to the observation space. Here, the intention was to exploit independence structure in MOMDPs for scalability and efficiency.

2 Background

A regular discrete-time Markov decision process (MDP) is a tuple $\mathcal{M} \doteq (\mathcal{S}, \mathcal{A}, \mathcal{R}, p, p_0)$, comprising: a *state space* \mathcal{S} , *action space* \mathcal{A} , and set of *rewards* $\mathcal{R} \subseteq \mathbb{R}$. The dynamics of the MDP are driven by an *initial state distribution* such that $s_0 \sim p_0(\cdot)$ and a stationary *transition kernel* where $(r_t, s_{t+1}) \sim p(\cdot, \cdot | s_t, \mathbf{a}_t)$ satisfies the Markov property, $p(r_t, s_{t+1} | h_t) = p(r_t, s_{t+1} | s_t, \mathbf{a}_t)$, for any history $h_t \doteq (s_0, \mathbf{a}_0, r_0, s_1, \dots, s_t, \mathbf{a}_t)$. Given an MDP, a (stochastic) policy, parameterised by $\theta \in \mathbb{R}^n$, is a mapping $\pi_\theta : \mathcal{S} \times \mathbb{R}^n \rightarrow \mathcal{P}(\mathcal{A})$ from states and weights to the set of probability measures on \mathcal{A} .

The conditional probability density of an action \mathbf{a} is denoted by $\pi_{\theta}(\mathbf{a} | s) \doteq \mathbb{P}(\mathbf{a} \in d\mathbf{a} | s, \theta)$ and we assume throughout that π_{θ} is continuously differentiable with respect to θ . For a given policy, the *return* starting from time t is defined as the discounted sum of future rewards, $G_t \doteq \sum_{k=0}^T \gamma^k r_{t+k+1}$, where $\gamma \in [0, 1]$ is the discount rate and T is the terminal time [42]. *Value functions* express the expected value of returns generated from a given state or state-action pair under the MDP's transition dynamics and policy π : that is, $v_{\pi}(s) \doteq \mathbb{E}_{\pi}[G_t | s_t = s]$ and $q_{\pi}(s, \mathbf{a}) \doteq \mathbb{E}_{\pi}[G_t | s_t = s, \mathbf{a}_t = \mathbf{a}]$. The objective in *control* is to find a policy that maximises v_{π} for all states with non-zero measure under p_0 , denoted by the Lebesgue integral $J(\theta) \doteq \mathbb{E}_{p_0}[v_{\pi_{\theta}}(s_0)] = \int_{\mathcal{S}} v_{\pi_{\theta}}(s_0) dp_0(s_0)$.

2.1 Policy Search

In this paper, we focus on policy gradient methods which optimise the parameters θ directly. This is achieved, in general, by performing gradient ascent on $J(\theta)$, for which Sutton et al. [43] derived

$$\nabla_{\theta} J(\theta) = \mathbb{E}_{\pi_{\theta}, \rho_{\pi_{\theta}}} [(q_{\pi_{\theta}}(s, \mathbf{a}) - b(s)) \mathbf{z}], \quad (1)$$

where $\mathbf{z} \doteq \nabla_{\theta} \ln \pi_{\theta}(\mathbf{a} | s)$ is the policy's score vector, $\rho_{\pi_{\theta}}(s) \doteq \int_{\mathcal{S}} \sum_{t=0}^{\infty} \gamma^t p(s_t = s | ds_0, \pi_{\theta})$ denotes the (improper) discounted-ergodic occupancy measure, and $b(s)$ is a state-dependent baseline (or, control variate) [33]. Here, $p(s_t = s | s_0, \pi_{\theta})$ is the probability of transitioning from $s_0 \rightarrow s$ in t steps under π_{θ} . Equation 1 is convenient for a number of reasons: 1. it is a score-based estimator [26]; and 2. it falls under the class of stochastic approximation algorithms [1]. This is important as it means $q_{\pi}(s, \mathbf{a})$ may be replaced by *any* unbiased quantity, say $\psi : \mathcal{S} \times \mathcal{A} \rightarrow \mathbb{R}$, such that $\mathbb{E}_{\pi, \rho_{\pi}}[\psi(s, \mathbf{a})] = q_{\pi}(s, \mathbf{a})$, while retaining convergence guarantees. It also implies that optimisation can be performed using stochastic gradient estimates, the standard variant of which is defined below.

Definition 2.1 (VPGs). The *vanilla policy gradient* estimator for target-baseline pair (ψ, b) is denoted

$$\mathbf{g}^V(s, \mathbf{a}) \doteq [\psi(s, \mathbf{a}) - b(s)] \mathbf{z}, \quad (2)$$

where $\nabla_{\theta} J(\theta) = \mathbb{E}_{\pi_{\theta}, \rho_{\pi_{\theta}}} [\mathbf{g}^V(s, \mathbf{a})]$.

2.2 Factored (Action-Space) MDPs

In this paper, we consider the class of MDPs in which the action-space factors into a product, $\mathcal{A} \doteq \bigotimes_{i=1}^n \mathcal{A}_i = \mathcal{A}_1 \times \cdots \times \mathcal{A}_n$, for some n . This is satisfied trivially when $n = 1$ and $\mathcal{A}_1 = \mathcal{A}$, but also holds in many common settings, such as $\mathcal{A} \doteq \mathbb{R}^n$, which factorises n times as $\bigotimes_{i=1}^n \mathbb{R}$. This is equivalent to requiring that actions, $\mathbf{a} \in \mathcal{A}$, are accessible in an elementwise fashion; without necessarily having \mathcal{A} be a vector space. For this purpose, we introduce the notion of partition maps which will be used throughout the paper.

Definition 2.2 (Partition Map). Define $\mathcal{X} \doteq \bigotimes_{i=1}^n \mathcal{X}_i$ and $J \subseteq [n]$ with $\mathcal{X}_J \doteq \bigotimes_{j \in J} \mathcal{X}_j$ such that a partition map (PM) for a pair (\mathcal{X}, J) is a function $\sigma : \mathcal{X} \rightarrow \mathcal{X}_J$ with complement $\bar{\sigma} : \mathcal{X} \rightarrow \mathcal{X}_{[n] \setminus J}$.

Partition maps are an extension of the canonical projections of the product topology, and are equivalent to the scope operator used by Tian et al. [47]. For example, if $(a_1, a_2, a_3) \doteq \mathbf{a} \in \mathcal{A} \doteq \mathbb{R}^3$ denotes a three-dimensional real action-space, then one possible PM is given by $\sigma(\mathbf{a}) = (a_1, a_3)$ with complement $\bar{\sigma}(\mathbf{a}) = (a_2)$. Note that there should always exist a unique inverse operation that recovers the original space; in this case, it would be expressed as $f((a_1, a_3), (a_2)) = (a_1, a_2, a_3)$.

3 Influence Networks

Consider an MOMDP with scalarised objective given by

$$J(\theta) \doteq \mathbb{E}_{p_0} \left[\psi(s, \mathbf{a}) \doteq \sum_{j=1}^m \lambda_j \psi_j(s, \sigma_j(\mathbf{a})) \right], \quad (3)$$

where $\lambda_j \in \mathbb{R}$ for all $1 \leq j \leq m$ and each $\psi_j(s, \sigma_j(\mathbf{a}))$ denotes some target that depends on a single partition of the action components. Traditional MDPs can be seen as a special case in which $m = 1$, and $\psi = \psi_1 \doteq q_{\pi}(s, \mathbf{a})$. The vector $\psi(s, \mathbf{a})$ comprises the concatenation of all m targets and each

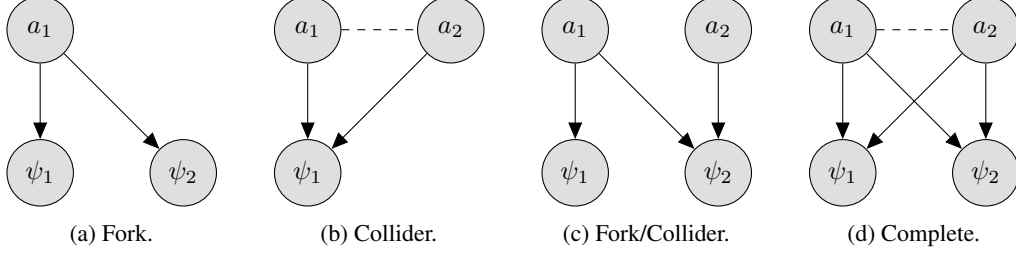


Figure 1: Influence network prototypes and action-target junction patterns [31, 32]. Edges depict dependencies between factors $a_i \in \mathcal{A}$ and targets $\psi_j \in \Psi$; and dashed lines a partition induced by the minimum factorisation.

partitioning is dictated by the *non-empty* maps $\sigma_j(\mathbf{a})$, the form of which is intrinsic to the MOMDP. For convenience, let us denote the collection of targets comprising $\psi(s, \mathbf{a})$ by

$$\Psi \doteq \{\psi_j : \psi(s, \mathbf{a}) = \langle \boldsymbol{\lambda}, \psi(s, \mathbf{a}) \rangle\}. \quad (4)$$

The intuition behind causal policy gradients is derived from the observation that each factor of the action-space only *influences* a subset of the m targets. Take, for example, Figure 1c which depicts an instance of a (causal) influence network between a 2-dimensional action vector and a 2-dimensional target. The edges suggest that a_1 affects the value of both ψ_1 and ψ_2 , whereas a_2 only affects ψ_2 . This corresponds to an objective of the form $\lambda_1 \psi_1(s, a_1) + \lambda_2 \psi_2(s, \mathbf{a})$, where each goal’s domain derives from the edges of the graph. This is formalised in Definition 3.1 below.

Definition 3.1 (Influence Network). A bipartite graph $\mathcal{G}(\mathcal{M}, \Psi) \doteq (I_{\mathcal{A}}, I_{\Psi}, E)$ is said to be the influence network of an MDP \mathcal{M} and target set Ψ if for $I_{\mathcal{A}} \doteq [|\mathcal{A}|]$ and $I_{\Psi} \doteq [|\Psi|]$, the presence of an edge, $e \in E$, between nodes $i \in I_{\mathcal{A}}$ and $j \in I_{\Psi}$ defines a causal relationship between the i^{th} factor of \mathcal{A} and the j^{th} target $\psi_j(s, \sigma_j(\mathbf{a}))$.

An influence network can be seen as a structural equation model [31] in which each vertex in $I_{\mathcal{A}}$ has a single, unique parent which is exogenous and drives the randomness in action sampling, and each vertex in I_{Ψ} has parents only in the set $I_{\mathcal{A}}$ as defined by the set of edges E . The structural equations along each edge $(i, j) \in E$ are given by the target functions themselves and the partition maps σ_j mirror the parents of each node j . Some examples of influence networks are illustrated in Figure 1; see also the appendix. We now define the key concept of influence matrices.

Definition 3.2 (Influence Matrix). Let $K_{\mathcal{G}}$ denote the *biadjacency matrix* of an influence network \mathcal{G} , defined as the $|I_{\mathcal{A}}| \times |I_{\Psi}|$ boolean matrix with $K_{ij} = 1 \iff (i, j) \in E$ for $i \in I_{\mathcal{A}}$ and $j \in I_{\Psi}$.

Together, these definitions form a calculus for expressing the causal relationships between the factors of an action-space and the targets of an objective of the form in Equation 3. We remark that, from an algorithmic perspective, we are free to choose between two representations: graph-based, or partition map-based. The duality between \mathcal{G} and K , and the set $\{\sigma_j : j \in I_{\Psi}\}$, is intrinsic to our choice of notation and serves as a useful correspondence during analysis.

3.1 Policy Factorisation

Influence networks capture the causal relationships between \mathcal{A} and Ψ , but policies are typically defined over groups of actions rather than the individual axes of \mathcal{A} . Consider, for example, a multi-asset trading problem in which an agent must quote buy and sell prices for each of n distinct assets [14, 40]. There is a natural partitioning between each pair of prices and the n sources of profit/loss, and one might therefore define the policy as a product of n bivariate distributions as opposed to a full joint, or fully factored model. This choice over *policy factorisation* relates to the independence assumptions we make on the distribution π_{θ} for the sake of performance. Indeed, in the majority of the literature, policies are defined using an isotropic distribution [56] since there is no domain knowledge to motivate more complex covariance structure. We formalise this below.

Definition 3.3 (Policy Factorisation). A *policy factorisation*, $\Sigma \doteq \{\sigma_i^{\pi} : i \in |\Sigma|\}$, is a set of disjoint partition maps that form a complete partitioning over the action space.

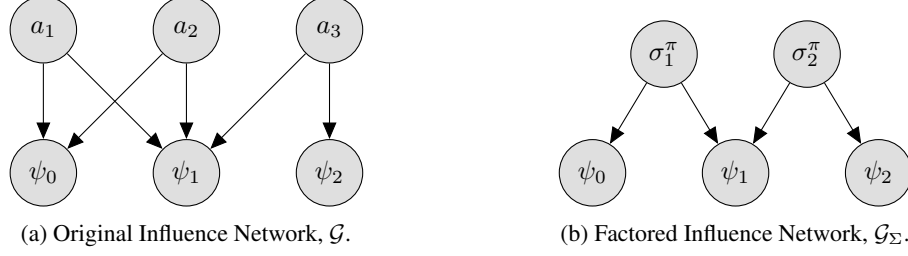


Figure 2: Influence network transformation under a Σ -factorisation with $\sigma_1^\pi(\mathbf{a}) \doteq (a_1, a_2)$ and $\sigma_2^\pi(\mathbf{a}) \doteq (a_3)$. Here, Σ corresponds to a minimum factorisation of the policy; i.e. $\Sigma = \Sigma^*$.

The definition above provides a means of expressing *any* joint policy distribution in terms of PMs,

$$\pi_\theta(\mathbf{a} | s) \doteq \prod_{i=1}^n \pi_{i,\theta}(\sigma_i^\pi(\mathbf{a}) | s), \quad (5)$$

where $\sigma_i^\pi \in \Sigma$ and $n = |\Sigma|$. This corresponds to a transformation of the underlying influence network where the action vertices are grouped under the n policy factors and, for any $i, j \in [n]$, $i \neq j$, we have mutual independence: $\sigma_i^\pi(\mathbf{a}) \perp\!\!\!\perp \sigma_j^\pi(\mathbf{a})$. This is captured in the following concept.

Definition 3.4 (Factored Influence Network). For a given influence network \mathcal{G} and policy factorisation Σ , we define a *factored influence network*, \mathcal{G}_Σ , by replacing $I_\mathcal{A}$ with I_Σ , the set of partitioned vertices, and merge the corresponding edges to give E_Σ . Similarly, denote by \mathbf{K}_Σ the influence matrix with respect to the Σ -factorisation.

Factored influence networks ascribe causal relationships between the policy factors in Equation 5 and the targets $\psi_j \in \Psi$. They play an important role in Section 4 and provide a refinement of Definition 3.1 which allows us to design more efficient algorithms. As an example, Figure 2 shows how one possible policy factorisation transforms an influence network \mathcal{G} into \mathcal{G}_Σ . Note that while the action nodes and edges have been partitioned into policy factors, the fundamental topology with respect to the attribution of influence remains unchanged; i.e. no dependencies are lost.

4 Causal Policy Gradients

Causal policy gradients exploit factored influence networks by attributing each $\psi_j \in \Psi$ only to the policy factors that were probabilistically responsible for generating it; that is, those with a connecting edge in the given \mathcal{G}_Σ . The intuition is that the extraneous targets in the objective do not contribute to learning, but do contribute towards variance. For example, it would be counter-intuitive to include ψ_2 of Figure 2b in the update for π_1 since it played no generative role. Naturally, by removing these terms from the gradient estimator, we can improve the signal to noise ratio and yield more stable algorithms. This idea can be formulated into a set of baselines which are defined and validated below.

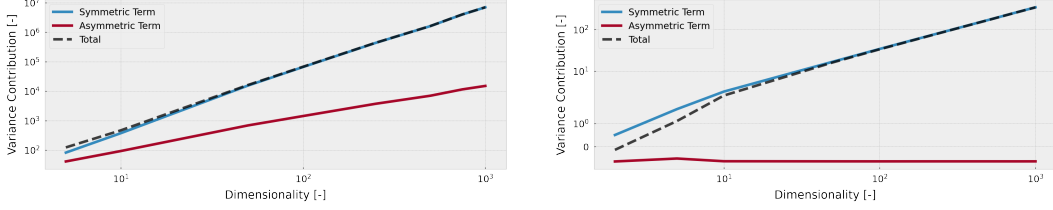
Definition 4.1 (Causal Baselines). For a given \mathcal{G}_Σ , the *causal baselines* (CBs) are defined as

$$b_i^C(s, \bar{\sigma}_i^\pi(\mathbf{a})) \doteq [(\mathbf{1} - \mathbf{K}_\Sigma) \boldsymbol{\lambda} \circ \boldsymbol{\psi}(s, \mathbf{a})]_i, \quad (6)$$

for all $i \in [|\Sigma|]$, where \circ denotes the Hadamard product and $\mathbf{1}$ is to be taken as an all-ones matrix.

Lemma 4.1. *Causal baselines are valid control variates if \mathcal{G}_Σ is true to the MDP (i.e. unbiased).*

Causal baselines are related to the action-dependent baselines studied by Wu et al. [56] and Tucker et al. [48], as well as the methods employed by COMA [9] and DRPGs [3] in multi-agent systems. Note, however, that CBs are distinct in two key ways: 1. they adhere to the structure of the influence network and account not only for policy factorisation, but also the target multiplicity of MOMDPs; and 2. unlike past work, the CBs were defined using an ansatz based on the structure implied by a given \mathcal{G}_Σ as opposed to explicitly deriving the arg min of the variance; see Appendix A. This means that, unlike optimal baselines, CBs can be computed efficiently and thus yield practical algorithms. Indeed, this very fact is why the state-value function is used so ubiquitously in traditional actor-critic methods as a state-dependent control variate despite being sub-optimal. It follows that we can define an analogous family of methods for MOMDPs with zero computational overhead.



(a) **Search bandit:** $\text{Cost}(\mathbf{a}) \doteq -\|\mathbf{a} - \mathbf{c}\|_1$ with fixed centroid vector $\mathbf{c} \in \mathbb{R}^n$. (b) **ReLU bandit:** $\text{Cost}(\mathbf{a}) \doteq -\sum_{i=1}^n \max(e_i a_i, 0)$ with fixed sign vector $\mathbf{e} \in \{-1, 1\}^n$.

Figure 3: Variance decomposition on a symmetric log scale for two bandit problems as a function of action-space dimensionality. Each term was computed using Monte-Carlo estimation with 10^5 samples and taking the arithmetic mean across all policy factors.

Proposition 1 (CPGs). Take a Σ -factored policy $\pi_\theta(\mathbf{a}|s)$ and $|\theta| \times |\Sigma|$ matrix of scores $\mathbf{S}(s, \mathbf{a})$. Then, for target vector $\psi(s, \mathbf{a})$ and multipliers λ , the CPG estimator

$$\mathbf{g}^C(s, \mathbf{a}) \doteq \mathbf{S}(s, \mathbf{a}) \mathbf{K}_\Sigma \lambda \circ \psi(s, \mathbf{a}), \quad (7)$$

is an unbiased estimator of the true policy gradient; i.e. $\nabla_\theta J(\theta) = \mathbb{E}_{\pi_\theta, \rho_{\pi_\theta}}[\mathbf{g}^C(s, \mathbf{a})]$.

Proposition 1 above shows that the VPG estimator given in Definition 2.1 can be expressed in our causal calculus as $\mathbf{S} \mathbf{1} \lambda \circ \psi$, where $\mathbf{1}$ is an all-ones matrix and, traditionally, $\psi \doteq q_\pi$; note that one can still include other baselines in Equation 7 such as v_π . In other words, *Proposition 1 strictly generalises the policy gradient theorem* [43] and, by virtue of its unbiasedness, thus retains all convergence guarantees. We also see that both COMA [9] and DRPGs [3] are special cases in which the influence network reflects the separation of agents with \mathbf{K}_Σ a square, and often diagonal matrix.

4.1 Variance Analysis

The variance reducing effect of causal baselines comprises two terms: 1. a symmetric and strictly non-negative component which scales with the *second moments* of b_i^C ; and 2. an asymmetric term which scales with the *expected values* of b_i^C . This is shown in the following result.

Proposition 2 (Variance Decomposition). Let \mathbf{g}_i denote a gradient estimate for the i^{th} factor of a Σ -factored policy π_θ (Equation 5). Then, $\Delta \mathbb{V}_i \doteq \mathbb{V}[\mathbf{g}_i^V] - \mathbb{V}[\mathbf{g}_i^C]$, satisfies

$$\Delta \mathbb{V}_i = \alpha_i \mathbb{E}_{\sigma_i^\pi(\mathbf{a})}[(b_i^C)^2] + 2\beta_i \mathbb{E}_{\sigma_i^\pi(\mathbf{a})}[b_i^C], \quad (8)$$

where $\mathbf{z}_i \doteq \nabla_\theta \ln \pi_{i,\theta}(\mathbf{a}|s)$, $\alpha_i \doteq \mathbb{E}_{\sigma_i^\pi(\mathbf{a})}[\langle \mathbf{z}_i, \mathbf{z}_i \rangle] \geq 0$ and $\beta_i \doteq \mathbb{E}_{\sigma_i^\pi(\mathbf{a})}[\langle \mathbf{z}_i, \mathbf{z}_i \rangle (\psi + b_i^C)]$.

The first of these two terms is a “free lunch” which removes the targets that are not causally related to each factor. The asymmetric term, on the other hand, couples the adjusted target with the entries that were removed by the baseline. This suggests that asymmetry and covariance can have a regularising effect in VPGs that is not present in CPGs — a manifestation of the properties of control variates [26]. Now, if we do not assume that the target functions are bounded, then the asymmetric term in Equation 8 can grow arbitrarily in either direction, but we typically require that rewards are restricted to some compact subset $\mathcal{R} \subset \mathbb{R}$ to avoid this. Below, we show that if a similar requirement holds for each target function — namely, that $\inf_{\mathcal{S}, \mathcal{A}} \psi_j$ is well defined for each $\psi_j \in \Psi$ — then we can always construct a set of mappings that constrain (8) to be non-negative without biasing the gradient.

Corollary 4.1 (Non-Negative Variance Reduction). Let $\psi(s, \mathbf{a})$ be of the form in Equation 3. If $\psi_j(s, \mathbf{a}) \geq \psi_j$ for all $(s, \mathbf{a}) \in \mathcal{S} \times \mathcal{A}$ and $j \in [m]$, with $|\psi_j| < \infty$, then there exists a linear translation, $\psi_i \rightarrow \psi_i - \sum_{j=1}^m \lambda_j \psi_j$, which leaves the gradient unbiased but yields $\Delta \mathbb{V}_i \geq 0$.¹

Interestingly, numerical experiments on a pair of continuum armed bandits suggest that this transformation is seldom necessary; see Figure 3. As the number of policy factors and targets grow, so

¹This inequality can be made strict if either $\alpha_i > 0$ or $\beta_i > 0$ — where the former equates to having a non-zero trace of the Fisher information matrix — and a small $\varepsilon > 0$ is added to the translation.

too does the potential discrepancy in magnitude between the symmetric and asymmetric terms in Equation 8. The symmetric term starts to dominate even for small $|\Sigma|$. This is particularly prevalent when the influence matrix \mathbf{K}_Σ is very sparse and the baselines have wide coverage over Ψ . In other words, applying causal baselines when the influence network is very dense or even complete will not yield tangible benefits (e.g. in Atari games), but applying them to a problem with a rich causal structure such as traffic networks will almost certainly yield a significant net reduction in variance.

Bias-Variance Trade-Off. It is important to note that, in real-world problems, one does not always know the exact structure of the influence network underling an MDP *ex ante*. This poses a challenge since incorrectly *removing* edges can introduce bias and thus constrain the space of solutions that can be found by CPGs. Note, however, that this may not always be a problem, since a small amount bias for a large reduction in variance can be desirable. Furthermore, one could leverage curriculum learning to train the policy on (presumed) influence networks with increasing connectedness over time. This trade-off between bias and variance is present in many machine learning settings, and depends strongly on the problem at hand; we explore empirically this in Section 5.2.

4.2 Minimum Factorisation

For many classes of fully-observable MDPs, any policy factorisation is theoretically viable: we can fully factor the policy such that each action dimension is independent of all others; or, at the other extreme, treat the policy as a full joint distribution over \mathbf{a} . This holds because, in many classes of (fully-observable) MDPs, there exists at least one deterministic optimal policy [54, 35]. The covariance acts as a driver of exploration, and it’s initial value only affects the rate of convergence.² As a result, most research uses an isotropic Gaussian with diagonal covariance to avoid the cost of matrix inversion. This poses an interesting question: is there an “optimal” policy factorisation, $\Sigma_{\mathcal{G}}^*$, associated with an influence network \mathcal{G} ? Below we offer a possible characterisation.

Definition 4.2 (Minimum Factorisation). A minimum factorisation (MF), $\Sigma_{\mathcal{G}}^*$, of an influence network, \mathcal{G} , is defined as the *minimum biclique vertex cover, disjoint amongst I_A* .

It follows from Definition 4.2 that for any $\Sigma_{\mathcal{G}}^*$, each $\sigma_i \in \Sigma_{\mathcal{G}}^*$ is a biclique (i.e. complete bipartite subgraph) of the original influence network \mathcal{G} , and that the bipartite dimension is equal to the number of policy factors. For example, one can trivially verify that Figure 2b is an MF of the original graph; see also the reductions in Figure 1. In essence, an MF describes a complete partitioning over action vertices where each group is a biclique and have the same set of outgoing edges. The “minimum” qualifier then ensures that the maximum number of nodes are included in each of these groups, a property which allows us to prove the following result:

Theorem 4.1. *The MF $\Sigma_{\mathcal{G}}^*$ always exists and is unique.*

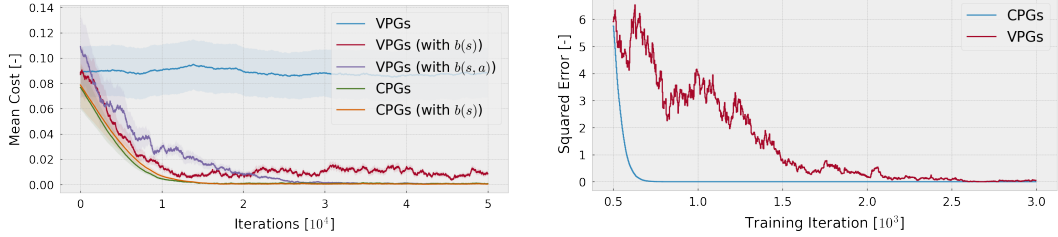
Minimum factorisation is highly intuitive and natural to the problem domains studied in this paper; see Section 5. It also yields factored policies which, generally, expose the minimum infimum bound on variance for a given influence network. This follows from the fact that an MF yields the greatest freedom to express covariance structure within each of the policy factors whilst also maximising the symmetric term in Equation 8. In fact, when each action corresponds to a single unique target, the MF enjoys a lower bound on variance that is linear in the number of factors. Finally, we remark that, whilst closely related to vertex covering problems (which are known to be NP-complete [18]), we observed experimentally that finding the MF can be done trivially in polynomial time [8].

5 Numerical Experiments

5.1 Search Bandits

Consider a continuum armed bandit with action space in \mathbb{R}^n and cost function: $\text{Cost}(\mathbf{a}) \doteq \|\mathbf{a} - \mathbf{c}\|_1 + \lambda \zeta(\mathbf{a})$, where $\mathbf{c} \in \mathbb{R}^n$, $\lambda \geq 0$ and $\zeta : \mathcal{A} \rightarrow \mathbb{R}_+$ is a penalty function. This describes a search problem in which the agent must locate the centroid \mathbf{c} subject to an action-regularisation penalty. It abstracts away the prediction aspects of MDP settings, and allows us to focus only on scalability; note that

²Note that this is not true in general: the policy’s covariance structure impacts the set of reachable solutions in partially-observable MDPs and stochastic games, for example.



(a) Convergence of CPGs (with and w/o additional state-dependent baseline) compared with VPGs using different baselines. The error bands denote the standard error on the mean over 10 random seeds. (b) Squared error between a_n and c_n during learning for the search bandit with $k = n - 1$.

Figure 4: Performance analysis of CPGs on the search bandit domain.

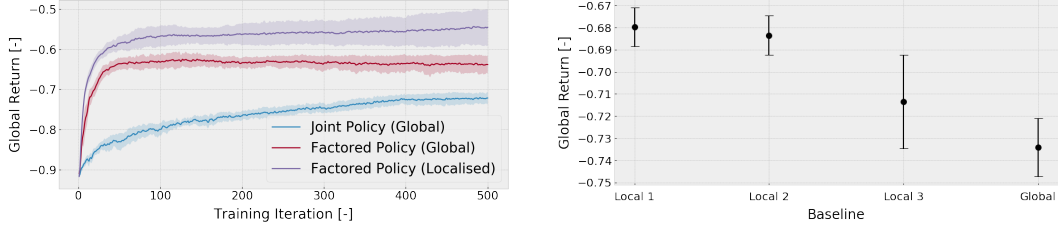
this problem is closely related to the bandit studied by Wu et al. [56] for the same purpose. In our experiments, the centroids were initialised with a uniform distribution, $c \sim \mathcal{U}(-5, 5)$ and were held fixed between episodes. The policy was defined as an isotropic Gaussian with fixed covariance, $\text{diag}(\mathbf{1})$, and initial location vector $\mu \doteq \mathbf{0}$. The influence network was specified such that each policy factor, $\pi_{i,\theta}$ for $i \in [n]$, used a reward target $\psi_i(\mathbf{a}) \doteq -\Delta_i(a_i) - \lambda\zeta(a_i)$, with $\Delta_i(a) \doteq |a - c_i|$, amounting to a collection of n forks (Figure 1a). The parameter vector, μ , was updated at each time step, and the hyperparameters are provided in Appendix D.

We began by examining the case where $\lambda = 0$ and the co-ordinate axes were fully decoupled. For this, Figure 7 compares the performance of CPGs and VPGs in terms of the average cost incurred during training. For VPGs, we note that stability was only possible without a baseline if an extremely low learning rate was used. Including a baseline dramatically improved performance, with the action-dependent case, $b(s, a)$, also leading to better asymptotic behaviour at the expense of a two orders of magnitude longer train-time according to the wall-clock compared with all other algorithms (VPGs and CPGs). In comparison, causal policy gradients, both with and without a learnt state-dependent baseline, yielded significantly reduced variance, leading to faster learning, more consistent convergence and highly robust asymptotic stability.

We then studied the impact of coupling terms in the cost function; i.e. $\lambda > 0$. For this, we considered a family of penalties taking the form of partially applied ℓ_2 norms: $\zeta_k(\mathbf{a}) \doteq \sqrt{\sum_{i=1}^k a_i^2}$, with $1 \leq k \leq n$. This set of functions allowed us to vary the penalty attribution across the n factors of \mathcal{A} . Figure 9 in the appendix, for example, demonstrates the performance advantage of CPGs for $k = n$ and $k = n/2$. In both cases, the improvement due to causal adjustment was found to be non-negative for every combination of learning rate and action space. This confirms that CPGs can indeed handle coupled targets and retains the variance reduction benefits that were explored in Section 4.1. As an illustrative example, consider the case where $k = n - 1$ and all but the last action dimension are subject to a penalty. This is a particularly challenging setting for VPGs because the magnitude of the combined cost function is much greater than $\Delta_n(a_n)$, leading to an *aliasing* of the final component of the action vector in the gradient. The result, as exemplified in Figure 4b, was that VPGs favoured reduction of overall error, and was therefore exposed to poor per-dimension performance; hence the increased noise in the a_n error process. CPGs avoid this effect by attributing gradients directly.

5.2 Traffic Networks

We now consider a classic traffic optimisation domain to demonstrate the scalability of our approach to large real-world problems. In particular, we consider variants of the (3×3) grid network benchmark environment — as originally proposed by Vinitzky et al. [50] — that is provided by the outstanding Flow framework [55, 21]. In this setting, the RL agent is challenged with managing a set of traffic lights with the objective of minimising the delay to vehicles travelling in the network; the configuration should be taken as identical unless explicitly stated. This requires a significant level of co-ordination, and indeed multi-agent approaches have shown exemplary performance in this space [50, 53]. However, much as with the search bandit, the probability of aliasing effects increases



(a) Convergence of joint/factored policies for the global reward, and using CPGs with the spatio-causal baseline. Each curve depicts the mean value across 5 random seeds with standard error bands.

(b) Performance degradation as a function of the n -level spatio-causal baseline approximation in a 2×6 grid network. Each point is the average terminal value across 5 seeds and with standard error bands.

Figure 5: Performance analysis of CPGs (with PPO and GAE) on the traffic network domain.

substantially with the number of lights/intersections; i.e. the dimensionality of the action-space. This affects both single- and multi-agent approaches when the global reward is used to optimise the policy.

To this end, we propose a causal “baseline” that *removes reward terms derived from streets/edges that are not directly connected to a given traffic light*. This is based on the hypothesis that the local problem is sufficiently isolated from the rest of the system that we may still find a (near)-optimal solution; much as with local-form models [27]. Of course, this could introduce bias at the cost of variance if we are incorrect (see Section 4.1), but this turns out to be an effective trade-off as exemplified in Figure 5a. In this plot we compare the performance of three policies learnt using PPO [38] and GAE [37] (with an additional state-dependent baseline): (1) a naïve joint policy over the 9-dimensional action-space and global reward; (2) a shared policy over the global reward; and (3) a shared policy using the local spatial baseline. The global reward in this case was defined as the negative of the mean delay introduced in the system minus a scaled penalty on vehicles at near standstill; see Appendix E for more details. As expected, we observe that the causal baseline improves learning efficiency, but, perhaps surprisingly, we also find that the *asymptotic behaviour is also superior*. We posit that this relates to the fact that, with a fixed learning rate, stochastic gradient descent cannot distinguish between points within a ball of the optimum solution with radius that scales with the variance on the estimator. In other words, significant reductions in variance, even if they introduce a small amount of bias, may increase the likelihood of reaching the true optimal solution by virtue of having much greater precision.

To better understand this trade-off, we also explored the impact of “expanding” the local causal baseline in a larger system of 2×6 intersections. With this new baseline we retain reward terms derived from lights up to n edges away in either the east or west directions. The variable n thus provides a dial to directly tweak the bias and variance of the policy gradient estimator (i.e. increasing n reduces bias but increases variance). The result, as shown in Figure 5b, suggest that performance decreases monotonically as a function of n . This corroborates the claim in Section 4.1 that introducing some bias in exchange for a reduction in variance can be a worthwhile trade-off in large problems.

6 Conclusion

Causal policy gradients derive from the observation that many MOMDPs exhibit redundancy in their reward structure. Here, we have characterised this phenomenon using causal graphs, and demonstrated that conditional independence between factors of the action-space and the optimisation targets can be exploited in the form of a causal baseline. The resulting family of algorithms subsume many existing approaches in the literature. Our results in large-scale bandit and concurrent traffic management problems suggest that CPGs are highly suited to real-world problems, and may provide a way of scaling RL to domains that have hitherto remained intractable. What’s more, CPGs are compatible with other techniques that improve policy gradient performance. For example, they can be extended to use natural gradients by pre-multiplying Equation 7 by the inverse Fisher information matrix [17], and can even use additional baselines to reduce variance even further, as in Section 5.2. In future work we intend to address the following interesting questions: (a) Can we infer/adapt the structure of influence networks? (b) Are there canonical structures within \mathcal{S} and \mathcal{K} ? (c) What theoretical insights can be derived from a more detailed analysis of the variance properties of CPGs? We argue

that factored approaches such as CPGs — which are complementary to ideas like influence-based abstraction [27] — are one of the most promising directions for practical RL. Addressing some of these questions, we believe, would thus be of great value to the community.

Acknowledgments and Disclosure of Funding

The authors would like to acknowledge our colleagues Joshua Lockhart, Jason Long and Rui Silva for their input and suggestions at various key stages of the research.

Disclaimer This paper was prepared for informational purposes by the Artificial Intelligence Research group of JPMorgan Chase & Co and its affiliates (“J.P. Morgan”), and is not a product of the Research Department of J.P. Morgan. J.P. Morgan makes no representation and warranty whatsoever and disclaims all liability, for the completeness, accuracy or reliability of the information contained herein. This document is not intended as investment research or investment advice, or a recommendation, offer or solicitation for the purchase or sale of any security, financial instrument, financial product or service, or to be used in any way for evaluating the merits of participating in any transaction, and shall not constitute a solicitation under any jurisdiction or to any person, if such solicitation under such jurisdiction or to such person would be unlawful.

© 2021 JPMorgan Chase & Co. All rights reserved.

References

- [1] Vivek S Borkar. *Stochastic Approximation: A Dynamical Systems Viewpoint*, volume 48. Springer, 2009.
- [2] Craig Boutilier, Thomas Dean, and Steve Hanks. Planning under uncertainty: Structural assumptions and computational leverage. In *Proceedings of the Second European Workshop on Planning*, pages 157–171, 1995.
- [3] Jacopo Castellini, Sam Devlin, Frans A Oliehoek, and Rahul Savani. Difference Rewards Policy Gradients. In *Proc. of AAMAS’21*, 2021.
- [4] Po-Wei Chou, Daniel Maturana, and Sebastian Scherer. Improving Stochastic Policy Gradients in Continuous Control with Deep Reinforcement Learning using the Beta Distribution. In *Proc. of ICML*, pages 834–843, 2017.
- [5] Elena Congeduti, Alexander Mey, and Frans A Oliehoek. Loss bounds for approximate influence-based abstraction. *arXiv preprint arXiv:2011.01788*, 2020.
- [6] Ivana Dusparic and Vinny Cahill. Autonomic Multi-Policy Optimization in Pervasive Systems: Overview and evaluation. *TAAS*, 7(1):1–25, 2012.
- [7] Carson Eisenach, Haichuan Yang, Ji Liu, and Han Liu. Marginal policy gradients: A unified family of estimators for bounded action spaces with applications. In *Proc. of ICLR*, 2019.
- [8] Herbert Fleischner, Egbert Mujuni, Daniël Paulusma, and Stefan Szeider. Covering Graphs with Few Complete Bipartite Subgraphs. *Theoretical Computer Science*, 410(21-23):2045–2053, 2009.
- [9] Jakob Foerster, Gregory Farquhar, Triantafyllos Afouras, Nantas Nardelli, and Shimon Whiteson. Counterfactual Multi-Agent Policy Gradients. In *Proc. of AAAI*, 2018.
- [10] Yasuhiro Fujita and Shin-ichi Maeda. Clipped Action Policy Gradient. In *Proc. of ICML*, pages 1597–1606, 2018.
- [11] Mohammad Ghavamzadeh, Shie Mannor, Joelle Pineau, and Aviv Tamar. Bayesian Reinforcement Learning: A Survey. *Foundations and Trends® in Machine Learning*, 8(5-6):359–483, 2015.
- [12] Will Grathwohl, Dami Choi, Yuhuai Wu, Geoff Roeder, and David Duvenaud. Backpropagation through the Void: Optimizing control variates for black-box gradient estimation. In *Proc. of ICLR*, 2018.

- [13] Evan Greensmith, Peter L Bartlett, and Jonathan Baxter. Variance Reduction Techniques for Gradient Estimates in Reinforcement Learning. *JMLR*, 5:1471–1530, 2004.
- [14] Olivier Guéant and Iuliia Manziuk. Deep Reinforcement Learning for Market Making in Corporate Bonds: Beating the Curse of Dimensionality. *Applied Mathematical Finance*, 26(5): 387–452, 2019.
- [15] Carlos Guestrin, Daphne Koller, Ronald Parr, and Shobha Venkataraman. Efficient Solution Algorithms for Factored MDPs. *JMLR*, 19:399–468, 2003.
- [16] Anderson Jonsson and Andrew Barto. Causal Graph Based Decomposition of Factored MDPs. *JMLR*, 7(11), 2006.
- [17] Sham M Kakade. A Natural Policy Gradient. *Proc. of NeurIPS*, 14:1531–1538, 2001.
- [18] Richard M Karp. Reducibility Among Combinatorial Problems. In *Complexity of Computer Computations*, pages 85–103. Springer, 1972.
- [19] Vijay R Konda and John N Tsitsiklis. Actor-Critic Algorithms. In *Proc. of NeurIPS*, pages 1008–1014, 2000.
- [20] Jae Won Lee and O Jangmin. A Multi-Agent Q-Learning Framework for Optimizing Stock Trading Systems. In *Proc. of DEXA*, pages 153–162. Springer, 2002.
- [21] Eric Liang, Richard Liaw, Robert Nishihara, Philipp Moritz, Roy Fox, Ken Goldberg, Joseph Gonzalez, Michael Jordan, and Ion Stoica. RLlib: Abstractions for Distributed Reinforcement Learning. In *Proc. of ICML*, pages 3053–3062, 2018.
- [22] Hao Liu, Yihao Feng, Yi Mao, Dengyong Zhou, Jian Peng, and Qiang Liu. Action-Dependent Control Variates for Policy Optimization via Stein Identity. In *Proc. of ICLR*, 2018.
- [23] Prashan Madumal, Tim Miller, Liz Sonenberg, and Frank Vetere. Explainable Reinforcement Learning Through a Causal Lens. In *Proc. of AAAI*, volume 34, pages 2493–2500, 2020.
- [24] Patrick Mannion, Sam Devlin, Jim Duggan, and Enda Howley. Reward shaping for knowledge-based multi-objective multi-agent reinforcement learning. *The Knowledge Engineering Review*, 33, 2018.
- [25] Shie Mannor and Nahum Shimkin. A Geometric Approach to Multi-Criterion Reinforcement Learning. *JMLR*, 5:325–360, 2004.
- [26] Shakir Mohamed, Mihaela Rosca, Michael Figurnov, and Andriy Mnih. Monte Carlo Gradient Estimation in Machine Learning. *JMLR*, 21(132):1–62, 2020.
- [27] Frans Oliehoek, Stefan Witwicki, and Leslie Kaelbling. Influence-Based Abstraction for Multiagent Systems. In *Proc. of AAAI*, volume 26, 2012.
- [28] Frans Oliehoek, Stefan Witwicki, and Leslie Kaelbling. A sufficient statistic for influence in structured multiagent environments. *Journal of Artificial Intelligence Research*, 70:789–870, 2021.
- [29] Matteo Papini, Damiano Binaghi, Giuseppe Canonaco, Matteo Pirodda, and Marcello Restelli. Stochastic Variance-Reduced Policy Gradient. In *Proc. of ICML*, pages 4026–4035, 2018.
- [30] Yagna Patel. Optimizing Market Making using Multi-Agent Reinforcement Learning. *arXiv preprint arXiv:1812.10252*, 2018.
- [31] Judea Pearl. *Causality*. Cambridge University Press, 2009.
- [32] Judea Pearl and Dana Mackenzie. *The Book of Why: The New Science of Cause and Effect*. Basic Books, 2018.
- [33] Jan Peters and Stefan Schaal. Policy Gradient Methods for Robotics. In *Proc. of IEEE/RSJ*, pages 2219–2225. IEEE, 2006.

- [34] LA Prashanth and Mohammad Ghavamzadeh. Variance-Constrained Actor-Critic Algorithms for Discounted and Average Reward MDPs. *Machine Learning*, 105(3):367–417, 2016.
- [35] Martin L Puterman. *[M]arkov Decision Processes: Discrete Stochastic Dynamic Programming*. John Wiley & Sons, 2014.
- [36] Diederik M Roijers, Peter Vamplew, Shimon Whiteson, and Richard Dazeley. A Survey of Multi-Objective Sequential Decision-Making. *JAIR*, 48:67–113, 2013.
- [37] John Schulman, Philipp Moritz, Sergey Levine, Michael Jordan, and Pieter Abbeel. High-Dimensional Continuous Control using Generalized Advantage Estimation. *arXiv preprint arXiv:1506.02438*, 2015.
- [38] John Schulman, Filip Wolski, Prafulla Dhariwal, Alec Radford, and Oleg Klimov. Proximal Policy Optimization Algorithms. *arXiv preprint arXiv:1707.06347*, 2017.
- [39] David Silver, Leonard Newnham, David Barker, Suzanne Weller, and Jason McFall. Concurrent Reinforcement Learning from Customer Interactions. In *Proc. of ICML*, pages 924–932, 2013.
- [40] Thomas Spooner and Rahul Savani. Robust Market Making via Adversarial Reinforcement Learning. In *Proc. of IJCAI*, pages 4590–4596, 7 2020. Special Track on AI in FinTech.
- [41] Miguel Suau, Elena Congeduti, Rolf Starre, Aleksander Czechowski, and Frans A Oliehoek. Influence-aware memory for deep reinforcement learning. *arXiv preprint arXiv:1911.07643*, 2019.
- [42] Richard S Sutton and Andrew G Barto. *Reinforcement Learning: An Introduction*. MIT Press, 2018.
- [43] Richard S Sutton, David A McAllester, Satinder P Singh, and Yishay Mansour. Policy Gradient Methods for Reinforcement Learning with Function Approximation. In *Proc. NeurIPS*, pages 1057–1063, 2000.
- [44] Aviv Tamar, Dotan Di Castro, Ron Meir, and Peter Dayan. Integrating a Partial Model into Model Free Reinforcement Learning. *JMLR*, 13(6), 2012.
- [45] Chen Tessler, Daniel J Mankowitz, and Shie Mannor. Reward Constrained Policy Optimization. In *Proc. of ICLR*, 2019.
- [46] Philip S Thomas and Emma Brunskill. Policy Gradient Methods for Reinforcement Learning with Function Approximation and Action-Dependent Baselines. *arXiv preprint arXiv:1706.06643*, 2017.
- [47] Yi Tian, Jian Qian, and Suvrit Sra. Towards Minimax Optimal Reinforcement Learning in Factored Markov Decision Processes. *Proc. of NeurIPS*, 33, 2020.
- [48] George Tucker, Surya Bhupatiraju, Shixiang Gu, Richard Turner, Zoubin Ghahramani, and Sergey Levine. The Mirage of Action-Dependent Baselines in Reinforcement Learning. In *Proc. of ICML*, volume 80, pages 5015–5024, 10–15 Jul 2018.
- [49] Kristof Van Moffaert, Tim Brys, Arjun Chandra, Lukas Esterle, Peter R Lewis, and Ann Nowé. A Novel Adaptive Weight Selection Algorithm for Multi-Objective Multi-Agent Reinforcement Learning. In *Proc. of IJCNN*, pages 2306–2314. IEEE, 2014.
- [50] Eugene Vinitsky, Aboudy Kreidieh, Luc Le Flem, Nishant Kheterpal, Kathy Jang, Cathy Wu, Fangyu Wu, Richard Liaw, Eric Liang, and Alexandre M Bayen. Benchmarks for reinforcement learning in mixed-autonomy traffic. In *Proc. of CoRL*, pages 399–409. PMLR, 2018.
- [51] Yuandou Wang, Hang Liu, Wanbo Zheng, Yunni Xia, Yawen Li, Peng Chen, Kunyin Guo, and Hong Xie. Multi-Objective Workflow Scheduling with Deep-Q-Network-Based Multi-Agent Reinforcement Learning. *Access*, 7:39974–39982, 2019.
- [52] Lex Weaver and Nigel Tao. The Optimal Reward Baseline for Gradient-Based Reinforcement Learning. In *Proc. of UAI*, pages 538–545, 2001.

- [53] Haoran Wei, Xuanzhang Liu, Lena Mashayekhy, and Keith Decker. Mixed-Autonomy Traffic Control with Proximal Policy Optimization. In *Proc. of VNC*, pages 1–8, 2019.
- [54] Marco Wiering and Martijn van Otterlo. *Reinforcement Learning: State-of-the-Art*, volume 12. Springer Science & Business Media, 2012.
- [55] Cathy Wu, Aboudy Kreidieh, Kanaad Parvate, Eugene Vinitsky, and Alexandre M Bayen. Flow: A modular learning framework for autonomy in traffic. *arXiv preprint arXiv:1710.05465*, 2017.
- [56] Cathy Wu, Aravind Rajeswaran, Yan Duan, Vikash Kumar, Alexandre M Bayen, Sham Kakade, Igor Mordatch, and Pieter Abbeel. Variance Reduction for Policy Gradient with Action-Dependent Factorized Baselines. In *Proc. of ICLR*, 2018.

A Causal Baselines

As shown in the main text, under the assumption that the influence network is unbiased, our causal baselines are indeed valid control variates. We prove this result below, repeating the statement itself for posterity and providing a supplementary lemma on control variates as a restatement of known results.

Lemma A.1 (Control Variate). *Let X , Y and Z be random variables where the law of X conditional on Z is denoted $\mathbb{P}_\theta(X|Z)$, and Y is independent of X conditioned on Z ; i.e. $X \perp\!\!\!\perp Y \mid Z$. Then, we have that $\mathbb{E}[Y \nabla_\theta \ln \mathbb{P}_\theta(X)] = 0$.*

Proof. The proof follows from the law of iterated expectations:

$$\begin{aligned} \mathbb{E}[Y \nabla_\theta \ln \mathbb{P}_\theta(X)] &= \mathbb{E}[\mathbb{E}[Y \nabla_\theta \ln \mathbb{P}_\theta(X) \mid Z]] = \mathbb{E}[\mathbb{E}[Y \mid Z] \mathbb{E}[\nabla_\theta \ln \mathbb{P}_\theta(X) \mid Z]] = 0, \\ \text{since } \mathbb{E}[\nabla_\theta \ln \mathbb{P}_\theta(X) \mid Z] &= 0. \end{aligned}$$

Lemma 4.1. *Causal baselines are valid control variates if \mathcal{G}_Σ is true to the MDP (i.e. unbiased).*

Proof. Consider an objective $J(\theta)$ of the form defined in Equation 3, a factored influence network \mathcal{G}_Σ and a Σ -factored policy $\pi_\theta(\mathbf{a} \mid s) \doteq \prod_{i=1}^n \pi_{i,\theta}(\sigma_i^\pi(\mathbf{a}) \mid s)$. Now, let us define a stochastic policy gradient estimator

$$\nabla_\theta J(\theta) = \mathbb{E}_{\pi_\theta, \rho_{\pi_\theta}} \left[\mathbf{g}(s, \mathbf{a}) \doteq \sum_{i=1}^n [\psi(s, \mathbf{a}) + b_i^C(s, \bar{\sigma}_i^\pi(\mathbf{a}))] \mathbf{z}_i \right],$$

where $\mathbf{z}_i \doteq \nabla_\theta \ln \pi_{i,\theta}(\sigma_i^\pi(\mathbf{a}) \mid s)$ and $b_i^C(s, \bar{\sigma}_i^\pi(\mathbf{a}))$ is the i^{th} causal baseline (see Definition 4.1). If \mathcal{G}_Σ is unbiased then we have mutual independence between each action partition and, since $b_i^C(s, \bar{\sigma}_i^\pi(\mathbf{a}))$ depends only on s and $\bar{\sigma}_i^\pi(\mathbf{a})$ — i.e. the action elements that are not in the support of $\pi_{i,\theta}$ — we can readily apply Lemma A.1, thus concluding the proof. ■

A.1 Optimality

In contrast to the causal baselines, solving for the optimal baseline in general is a non-trivial challenge. Indeed, the results presented by Wu et al. [56] rely on a key assumption that the policy factors do not share parameters in order to simplify the analysis; i.e. that $\langle \mathbf{z}_i, \mathbf{z}_j \rangle \approx 0$ for any $i, j \in [|\Sigma|]$. Below we explain why this is a difficult problem, and leave it to future work to find the solution.

For notational convenience, let $\mathbf{g}(s, \mathbf{a}) \doteq \sum_{i=1}^n \mathbf{g}_i(s, \mathbf{a})$ such that the total variance on the gradient is given by

$$\mathbb{V}[\mathbf{g}(s, \mathbf{a})] = \sum_{i=1}^n \sum_{j=1}^n \text{Cov}[\mathbf{g}_i(s, \mathbf{a}), \mathbf{g}_j(s, \mathbf{a})]. \quad (9)$$

The n *optimal baselines* are given by the values that minimise Equation 9; i.e. $b_i^*(s, \bar{\sigma}_i^\pi(\mathbf{a})) \doteq \arg \min_{b_i} \mathbb{V}[\mathbf{g}(s, \mathbf{a})]$ for all $i \in [n]$. To solve this problem, we first apply the causal baseline decomposition such that $b_i^*(s, \bar{\sigma}_i^\pi(\mathbf{a})) = b_i^V(s, \bar{\sigma}_i^\pi(\mathbf{a})) + b_i^C(s, \bar{\sigma}_i^\pi(\mathbf{a}))$. This implies that the optimisation problem can be reduced to finding $\arg \min_{b_i^V} \mathbb{V}[\mathbf{g}(s, \mathbf{a})]$ when b_i is replaced with b_i^* for all $i \in [n]$. Now, let $\mathbf{x}_i \doteq [\mathbf{K}_\Sigma \psi(s, \mathbf{a})]_i \mathbf{z}_i$ and $\mathbf{y}_i \doteq b_i^V(s, \bar{\sigma}_i^\pi(\mathbf{a})) \mathbf{z}_i$ such that $\mathbf{g}_i(s, \mathbf{a}) = \mathbf{x}_i + \mathbf{y}_i$. Note that while \mathbf{y}_i depends on the full action, \mathbf{x}_i depends only on the actions influencing the targets in $[\mathbf{K}_\Sigma \psi(s, \mathbf{a})]_i$. Removing terms that are independent of b_i^V thus yields the following:

$$\begin{aligned} \arg \min_{b_i^V} \mathbb{V}[\mathbf{g}] &= \arg \min_{b_i^V} \left\{ \mathbb{V}[\mathbf{g}] + \sum_{j \neq i}^n \text{Cov}[\mathbf{g}_i, \mathbf{g}_j] \right\}, \\ &= \arg \min_{b_i^V} \left\{ \mathbb{V}[\mathbf{x}_i] + \mathbb{V}[\mathbf{y}_i] + 2 \text{Cov}[\mathbf{x}_i, \mathbf{y}_i] + \sum_{j \neq i}^n \text{Cov}[\mathbf{x}_i, \mathbf{x}_j] + \text{Cov}[\mathbf{x}_i, \mathbf{y}_j] + \text{Cov}[\mathbf{y}_i, \mathbf{x}_j] + \text{Cov}[\mathbf{y}_i, \mathbf{y}_j] \right\} \\ &= \arg \min_{b_i^V} \left\{ \mathbb{V}[\mathbf{y}_i] + 2 \text{Cov}[\mathbf{x}_i, \mathbf{y}_i] + \sum_{j \neq i}^n \text{Cov}[\mathbf{x}_i, \mathbf{y}_j] + \text{Cov}[\mathbf{y}_i, \mathbf{x}_j] + \text{Cov}[\mathbf{y}_i, \mathbf{y}_j] \right\}. \end{aligned}$$

To solve the equation above, we first expand each component and remove any redundant terms. For the variance on \mathbf{y}_i , we have that

$$\begin{aligned}
\mathbb{V}[\mathbf{y}_i] &= \mathbb{E}_{\mathbf{a}} \left[(b_i^V)^2 \langle \mathbf{z}_i, \mathbf{z}_i \rangle \right] + \langle \mathbb{E}_{\mathbf{a}} [b_i^V \mathbf{z}_i], \mathbb{E}_{\mathbf{a}} [b_i^V \mathbf{z}_i] \rangle, \\
&= \mathbb{E}_{\mathbf{a}} \left[(b_i^V)^2 \langle \mathbf{z}_i, \mathbf{z}_i \rangle \right] + \langle \mathbb{E}_{\sigma_i^\pi(\mathbf{a})} [b_i^V], \mathbb{E}_{\sigma_i^\pi(\mathbf{a})} [\mathbf{z}_i], \mathbb{E}_{\sigma_i^\pi(\mathbf{a})} [b_i^V], \mathbb{E}_{\sigma_i^\pi(\mathbf{a})} [\mathbf{z}_i] \rangle, \\
&= \mathbb{E}_{\mathbf{a}} \left[(b_i^V)^2 \langle \mathbf{z}_i, \mathbf{z}_i \rangle \right], \\
&= \mathbb{E}_{\sigma_i^\pi(\mathbf{a})} [\langle \mathbf{z}_i, \mathbf{z}_i \rangle] \mathbb{E}_{\sigma_i^\pi(\mathbf{a})} \left[(b_i^V)^2 \right].
\end{aligned} \tag{10}$$

It follows from this analysis that the covariance between \mathbf{y}_i and \mathbf{y}_j for any $i, j \in [\Sigma]$, with $i \neq j$, is given by

$$\text{Cov}[\mathbf{y}_i, \mathbf{y}_j] = \mathbb{E}_{\mathbf{a}} [b_i^V b_j^V \langle \mathbf{z}_i, \mathbf{z}_j \rangle]. \tag{11}$$

Finally, we can expand the covariance between \mathbf{x}_i and \mathbf{y}_i ,

$$\begin{aligned}
\text{Cov}[\mathbf{x}_i, \mathbf{y}_i] &= \mathbb{E}_{\mathbf{a}} [\langle \mathbf{K}_\Sigma \boldsymbol{\psi} \rangle_i b_i^V \langle \mathbf{z}_i, \mathbf{z}_i \rangle] + \langle \mathbb{E}_{\mathbf{a}} [\langle \mathbf{K}_\Sigma \boldsymbol{\psi} \rangle_i \mathbf{z}_i], \mathbb{E}_{\mathbf{a}} [b_i^V \mathbf{z}_i] \rangle, \\
&= \mathbb{E}_{\mathbf{a}} [\langle \mathbf{K}_\Sigma \boldsymbol{\psi} \rangle_i b_i^V \langle \mathbf{z}_i, \mathbf{z}_i \rangle] + \langle \mathbb{E}_{\mathbf{a}} [\langle \mathbf{K}_\Sigma \boldsymbol{\psi} \rangle_i \mathbf{z}_i], \mathbb{E}_{\sigma_i^\pi(\mathbf{a})} [b_i^V] \mathbb{E}_{\sigma_i^\pi(\mathbf{a})} [\mathbf{z}_i] \rangle, \\
&= \mathbb{E}_{\mathbf{a}} [\langle \mathbf{K}_\Sigma \boldsymbol{\psi} \rangle_i b_i^V \langle \mathbf{z}_i, \mathbf{z}_i \rangle], \\
&= \mathbb{E}_{\sigma_i^\pi(\mathbf{a})} [b_i^V] \mathbb{E}_{\sigma_i^\pi(\mathbf{a})} [\langle \mathbf{K}_\Sigma \boldsymbol{\psi} \rangle_i \langle \mathbf{z}_i, \mathbf{z}_i \rangle],
\end{aligned} \tag{12}$$

and similarly resolve the cross-covariance terms:

$$\text{Cov}[\mathbf{x}_i, \mathbf{y}_j] = \langle \mathbb{E}_{\sigma_i^\pi(\mathbf{a})} [b_i^V \mathbf{z}_i], \mathbb{E}_{\sigma_j^\pi(\mathbf{a})} [\langle \mathbf{K}_\Sigma \boldsymbol{\psi} \rangle_j \mathbf{z}_j] \rangle. \tag{13}$$

The quantities above provide us with a platform to find solutions. For example, the optimal baseline approximation proposed by Wu et al. [56] can be found if we assume that $\langle \mathbf{z}_i, \mathbf{z}_j \rangle \approx 0$ since Equation 11 and Equation 12 go to zero. However, in the general case the problem is not quite so simple. The reason for this is that the baselines interact via the cross-covariance term in Equation 11. As a result, we cannot solve for each b_i^V independently of the others. Instead, we have a system of polynomial equations which may not have a unique solution. In fact, since each equation has degree $d = 2$, it follows the number of solutions can be as large $d^{|\Sigma|}$. In general, there are very few methods that can solve these type of systems, and those that can are limited to bounds of approximately $d^{|\Sigma|} \approx 20$. It seems reasonable to assume that any solution, while viable, would be computationally impractical, but we leave it to future work to establish this result formally.

B Causal Policy Gradients

The validity of causal baselines, as shown in the previous section, extends to policy gradient themselves. As discussed in the main text, we can show that CPGs are unbiased and satisfy certain variance bounds compared with conventional policy gradients. We restate the original propositions below and provide the proofs in full.

Proposition 1. *Take a Σ -factored policy $\pi_\theta(\mathbf{a}|s)$ and $|\theta| \times |\Sigma|$ matrix of scores $\mathbf{S}(s, \mathbf{a})$. Then, for target vector $\boldsymbol{\psi}(s, \mathbf{a})$ and multipliers $\boldsymbol{\lambda}$, the CPG estimator*

$$\mathbf{g}^C(s, \mathbf{a}) \doteq \mathbf{S}(s, \mathbf{a}) \mathbf{K}_\Sigma \boldsymbol{\lambda} \circ \boldsymbol{\psi}(s, \mathbf{a}),$$

is an unbiased estimator of the true policy gradient; i.e. $\nabla_\theta J(\theta) = \mathbb{E}_{\pi_\theta, \rho_{\pi_\theta}} [\mathbf{g}^C(s, \mathbf{a})]$.

Proof. Let \mathcal{G}_Σ denote an Σ -factored influence network with policy $\pi_\theta(\mathbf{a}|s) \doteq \prod_{i=1}^n \pi_{i,\theta}(\sigma_i^\pi(\mathbf{a})|s)$, and global target function $\psi(s, \mathbf{a}) = \sum_{j=1}^m \lambda_j \psi_j(s, \sigma_j(\mathbf{a})) = \langle \boldsymbol{\lambda}, \boldsymbol{\psi}(s, \mathbf{a}) \rangle$. The score matrix, $\mathbf{S}(s, \mathbf{a}) \doteq [\mathbf{z}_1^\top, \dots, \mathbf{z}_n^\top]^\top$, then has size $|\theta| \times n$, where $\mathbf{z}_i \doteq \nabla_\theta \ln \pi_{i,\theta}(\sigma_i^\pi(\mathbf{a})|s)$. From this we can express the conventional policy gradient with no baseline as the linear product $\mathbf{g}(s, \mathbf{a}) = \mathbf{S}(s, \mathbf{a}) \mathbf{J}_{n,m} \boldsymbol{\psi}(s, \mathbf{a})$, where $\mathbf{J}_{n,m}$ is the $n \times m$ all-ones matrix. By Lemma 4.1 the causal baselines, $[(1 - \mathbf{K}_\Sigma) \boldsymbol{\psi}(s, \mathbf{a})]_i$, are valid control variates and thus have expected value of zero under π . This means that they can be subtracted without introducing bias in the policy gradient, yielding

$$\mathbf{g}(s, \mathbf{a}) = \underbrace{\mathbf{S}(s, \mathbf{a}) \mathbf{J}_{n,m} \boldsymbol{\psi}(s, \mathbf{a})}_{\text{Vanilla PG}} - \underbrace{\mathbf{S}(s, \mathbf{a}) (1 - \mathbf{K}_\Sigma) \boldsymbol{\psi}(s, \mathbf{a})}_{\text{Causal Correction}} = \mathbf{S}(s, \mathbf{a}) \mathbf{K}_\Sigma \boldsymbol{\psi}(s, \mathbf{a}).$$

It follows that $\nabla_{\theta} J(\theta) = \mathbb{E}_{\pi_{\theta}, \rho_{\pi_{\theta}}} [\mathbf{g}^C(s, \mathbf{a})]$ since $\mathbb{E}_{\pi_{\theta}, \rho_{\pi_{\theta}}} [\mathbf{g}^V(s, \mathbf{a})] = \mathbb{E}_{\pi_{\theta}, \rho_{\pi_{\theta}}} [\mathbf{g}^C(s, \mathbf{a})]$ which concludes the proof. ■

Proposition 2. Let \mathbf{g}_i denote a gradient estimate for the i^{th} factor of a Σ -factored policy π_{θ} (Equation 5). Then, $\Delta \mathbb{V}_i \doteq \mathbb{V}[\mathbf{g}_i^V] - \mathbb{V}[\mathbf{g}_i^C]$, satisfies

$$\Delta \mathbb{V}_i = \alpha_i \mathbb{E}_{\sigma_i^{\pi}(\mathbf{a})} \left[(b_i^C)^2 \right] + 2\beta_i \mathbb{E}_{\sigma_i^{\pi}(\mathbf{a})} [b_i^C],$$

where $\mathbf{z}_i \doteq \nabla_{\theta} \ln \pi_{i,\theta}(\mathbf{a} | s)$, $\alpha_i \doteq \mathbb{E}_{\sigma_i^{\pi}(\mathbf{a})} [\langle \mathbf{z}_i, \mathbf{z}_i \rangle] \geq 0$ and $\beta_i \doteq \mathbb{E}_{\sigma_i^{\pi}(\mathbf{a})} [\langle \mathbf{z}_i, \mathbf{z}_i \rangle (\psi + b_i^C)]$.

Proof. First, let us denote by \mathbf{X} and \mathbf{Y} two (possibly dependent) random variables, with $\mathbf{Z} \doteq \mathbf{X} - \mathbf{Y}$ such that

$$\begin{aligned} \Delta \mathbb{V} &\doteq \mathbb{V}[\mathbf{X}] - \mathbb{V}[\mathbf{Y}] = \mathbb{V}[\mathbf{Z} + \mathbf{Y}] - \mathbb{V}[\mathbf{Y}], \\ &= \mathbb{V}[\mathbf{Z}] + \mathbb{V}[\mathbf{Y}] + 2\text{Cov}[\mathbf{Y}, \mathbf{Z}] - \mathbb{V}[\mathbf{Y}], \\ &= \mathbb{V}[\mathbf{Z}] + 2\text{Cov}[\mathbf{Y}, \mathbf{Z}]. \end{aligned}$$

From Proposition 1, we can express the vanilla and causal policy gradient estimators for the i^{th} factor as $\psi \mathbf{S}_{:,i}$ and $(\psi - b_i^C) \mathbf{S}_{:,i}$, respectively, where the function arguments have been omitted for clarity. Assigning these values to \mathbf{X} and \mathbf{Y} we arrive at the equality relations

$$\begin{aligned} \mathbb{V}[\mathbf{Z}] &= \mathbb{V}[b_i^C \mathbf{z}_i] = \mathbb{E}_{\pi} \left[\langle \mathbf{z}_i, \mathbf{z}_i \rangle (b_i^C)^2 \right] \\ \text{Cov}[\mathbf{Y}, \mathbf{Z}] &= \text{Cov}[(\psi - b_i^C) \mathbf{z}_i, b_i^C \mathbf{z}_i] = \mathbb{E}_{\pi} [\langle \mathbf{z}_i, \mathbf{z}_i \rangle (\psi - b_i^C) b_i^C]. \end{aligned}$$

The former follows from the fact that $\mathbb{E}_{\pi}[\mathbf{S}_{:,i}] = 0$ for all i , and latter by noting that $\mathbb{E}[\mathbf{Z}] = 0$ due to Lemma 4.1. We can now exploit the independencies implied by the influence network, \mathcal{G}_{Σ} , to give

$$\Delta \mathbb{V}_i = \mathbb{E}_{\sigma_i^{\pi}(\mathbf{a})} [\langle \mathbf{z}_i, \mathbf{z}_i \rangle] \mathbb{E}_{\sigma_i^{\pi}(\mathbf{a})} \left[(b_i^C)^2 \right] + 2\mathbb{E}_{\sigma_i^{\pi}(\mathbf{a})} [\langle \mathbf{z}_i, \mathbf{z}_i \rangle (\psi - b_i^C)] \mathbb{E}_{\sigma_i^{\pi}(\mathbf{a})} [b_i^C],$$

This is the desired result and thus concludes the proof. ■

Corollary 4.1. Let $\psi(s, \mathbf{a})$ be of the form in Equation 3. If $\psi_j(s, \mathbf{a}) \geq \underline{\psi}_j$ for all $(s, \mathbf{a}) \in \mathcal{S} \times \mathcal{A}$ and $j \in [m]$, with $|\underline{\psi}_j| < \infty$, then there exists a linear translation, $\psi_i \rightarrow \psi_i - \sum_{j=1}^m \lambda_j \underline{\psi}_j$, which leaves the gradient unbiased but yields $\Delta \mathbb{V}_i \geq 0$.

Proof. Take a target set Ψ and let $\underline{\psi}_j \doteq \inf_{\mathcal{S}, \mathcal{A}} \psi_j$ for each $\psi \in \Psi$. The unbiasedness claim follows from the fact that these terms go to zero in expectation when weighted by the score functions; they are constants. The variance claim is also trivial, since $\psi_j + \sum_{k=1}^m \lambda_k \inf_{\mathcal{S}, \mathcal{A}} \psi_k$ are non-negative and, due to the summation over all $k \in [m]$, no CB can yield a negative value. Each term in Equation 8 (Proposition 2) must also be non-negative, which concludes the proof. ■

C Minimum Factorisation

The minimum factorisation of an influence network provides a natural way of partitioning action nodes into independent policy distributions. In the main text it was also stated that such a characterisation is theoretically grounded. We repeat this result below and provide the proof herein.

Theorem 4.1. The MF $\Sigma_{\mathcal{G}}^*$ always exists and is unique.

Proof. Bipartite graphs always have at least one valid biclique and thus MF. Now, for uniqueness, let \mathcal{G} denote an influence network. If \mathcal{G} is complete, then we automatically satisfy the uniqueness property since the MF will contain a single biclique that covers all vertices in $I_{\mathcal{A}}$. If \mathcal{G} is incomplete, then the proof can be shown through contradiction. Suppose that A and B are both MFs and therefore correspond to minimum biclique vertex covers, disjoint amongst $I_{\mathcal{A}}$. We know then that A and B must have the same dimensionality since they are optimal — i.e. contain the same number of bicliques — but, if they are distinct, then there must also exist at least one biclique $a \in A$ that is not in B . Since both MFs are defined over the same graph \mathcal{G} , the elements of a must be distributed between at least 2 distinct bicliques in B . However, if this is the case, the union of these subgraphs would also form a valid biclique. The new cover, B' , containing the merged bicliques is valid and has dimensionality $|B'| < |B| = |A|$. This implies that neither A nor B can be MFs. Since the same must be true for any A and B , it follows that there can be only one MF, thus concluding the proof. ■

D Search Bandit

The search bandit was designed to exhibit an influence network as illustrated in Figure 6. Below we summarise the hyperparameters for the two key experiments — namely the baseline comparison (BC) and aliasing demonstration (AD):

BC All algorithms were trained using a learning rate of 0.5 except for VPGs w/o a baseline which was only stable with a step size of 0.001. The state-based (i.e. scalar) baselines, $b(s) = b$, were trained using temporal-difference methods with a learning rate of 0.1. The action-dependent baseline, $b(s, a) \doteq -\|a - w\|_1 / |\mathcal{A}|$, was similarly trained using SARSA with a learning rate of 0.1.³ An additional 1000 episodes were also used at the start of each run to pre-train the baseline if used.

AD In the aliasing experiment, both VPGs and CPGs were trained for a 100-dimensional action-space with a regularisation penalty of $\lambda = 0.01$ on the first 99 action-components. VPGs were instantiated with a learning rate of 0.001, and CPGs with a rate of 0.01.

Additional results. In addition to the results presented in the paper, we also include Figures 7-9. These explore the impact of the causal baseline across a set of dimensionalities and learning rates. We show that VPGs are very sensitive to the learning rate, especially when $|\mathcal{A}|$ is large. CPGs, on the other hand, converge on the optimal solution consistently regardless of the problem instance. Similarly, we show that the mean number of steps required to reach such a solution for a finite budget is much lower for CPGs compared with VPGs.

Implications for MDPs. The search bandit is an interesting problem environment because, in many ways, it can emulate the learning process in arbitrary MDPs. This follows because, without loss of generality, we can always transform an MDP into a (possibly infinite) set of continuum multi-armed bandits, one occupying every unique state $s \in \mathcal{S}$. The question is how to define the cost function in order to achieve some form of equivalence. For example, if we consider deterministic policies, then we can clearly define the cost to be $\text{Cost}(a) \doteq \|a - \pi^*(s)\|_p$, for $p \geq 1$, and have the same solution set as given under Bellman optimality. This implies that the performance observed in the search bandit is likely to tell us about the performance in full MDPs. The results presented in Section 5.1 may thus provide evidence that CPGs will outperform VPGs for arbitrarily challenging MDPs.

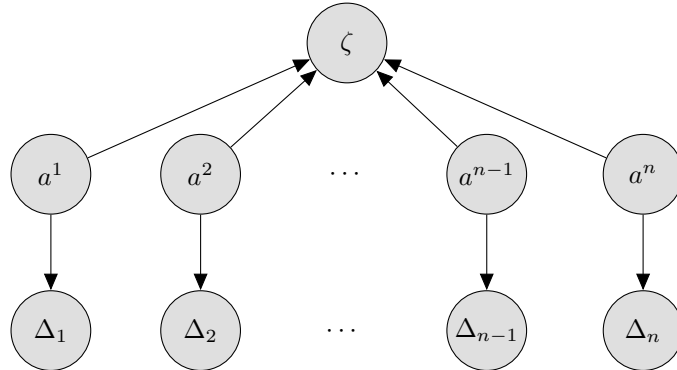


Figure 6: Influence network of the search bandit problem with optional coupling term.

E Traffic Systems

The traffic experiment were kept as close as possible to the benchmark specification for the grid problem provided by Flow [55]. In particular, we based the code of the “examples/exp_configs/rl/multiagent/multiagent_traffic_light_grid.py” and “examples/exp_configs/rl/signleagent/singleagent_traffic_light_grid.py” files on commit ID 4e47f7a. The

³In this formalism we only have sub-derivatives. For simplicity we simply assigned the gradient when a given action was equal to the weight.

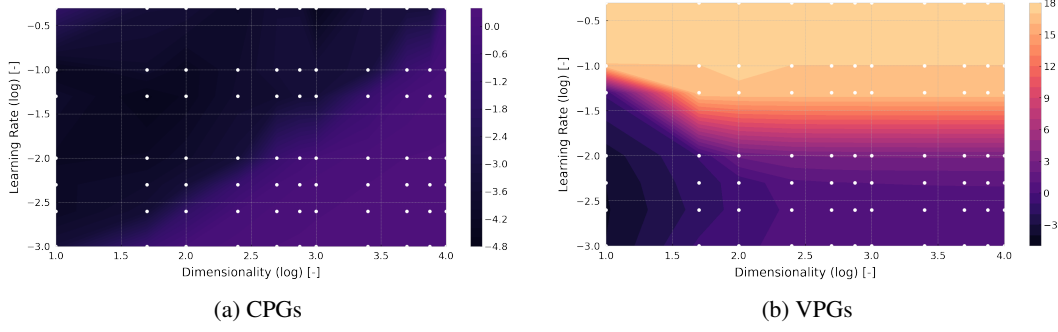


Figure 7: Mean optimality gap after 2×10^5 training iterations. The z -axis is given in a log scale and each point was computed from 16 random samples under the assumption of a Gamma distribution (optimality gap is lower bounded at zero).

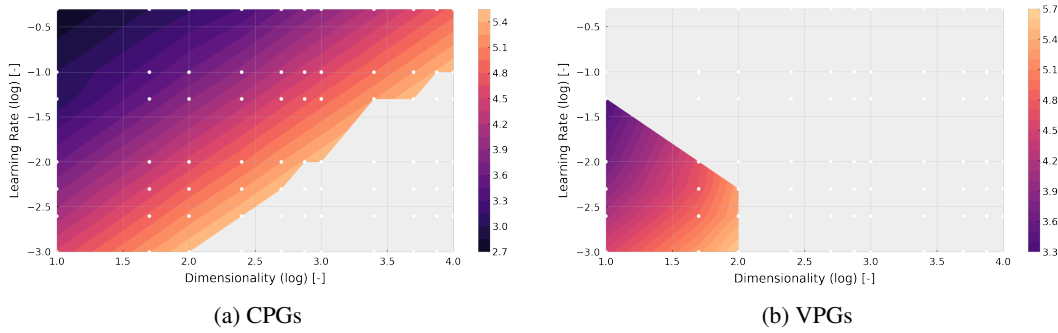


Figure 8: Mean number of time steps required to reach an optimality gap of 0.1, up to a limit of 5×10^5 training iterations; see Figure 7. The z -axis is given in a log scale, and unfilled (grey) regions depict either divergence or a failure to terminate in the allotted time. Each point was computed from 16 random samples under the assumption of a Gamma distribution (time is lower bounded at zero).

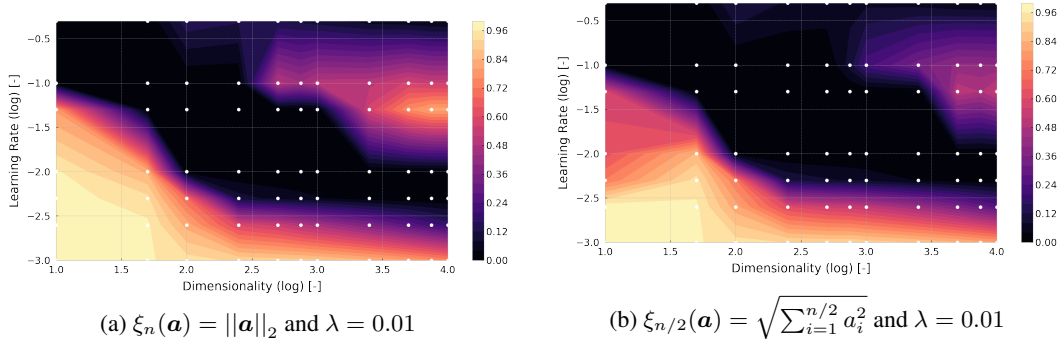


Figure 9: Ratio between the mean optimality gaps for CPGs over VPGs after 2×10^5 training iterations. Smaller values indicate that CPGs achieved a lower error relative to VPGs. Each point is the ratio of the two means, each computed using 16 random samples under the assumption of a Gamma distribution (optimality gaps are lower bounded at zero).

only changes that were made were to update the topology of the grid (i.e. 3×3 and 2×6), and to unify the reward function. We outline all the specific details below.

Reward functions. In order to unify the reward function across domains we implemented a custom variant of the “mean delay” case that worked for single- or multi-agent approaches. In particular, we changed the summation to only consider a subset of the edges in the network which allowed for localised computation. This can be done very easily in the Flow framework.

Traffic system parameters. The traffic intersection problem was instantiated with either a 3×3 topology, or a 2×6 topology, depending on the experiment. In all cases, an edge inflow of 300 was used, with initial speed of 30. The inner edges were given a length of 300, with the final edge in a route having length 100, and starting edge having length 300. Cars were created using the `SimCarFollowingController`, and `SumoCarFollowingParams` with a minimum gap of 2.5, maximum speed of 30, deceleration rate of 7.5 and “right of way” speed mode. The environment itself was initialised with target velocity of 50, switch time of 3, number of locally observed cars at 2, “actuated” TL type, and 4 locally observed edges.

Learning hyperparameters. In all cases we leveraged RLLIB’s implementation of PPO with GAE [21] using discount factor of 0.999, a Monte-Carlo interpolation rate of $\lambda = 0.97$, KL-target of 0.02, value function clipping bound at 10^4 , and learning rate of 5×10^{-4} . The policy was parameterised using a three-layer neural network with 32 units at each of the three hidden layers. A total of 50 CPUs were used, each generating a single rollout at each iteration with a horizon of 400 steps.